Supporting Information

Choi et al. 10.1073/pnas.1014154108

SI Materials and Methods

Experimental Autoimmune Encephalomyelitis Induction by Adoptive Transfer. Mice were immunized with myelin oligodendrocyte glycoprotein (MOG) amino acid 35–55 (1); 14 d postimmunization, lymph node (LN) cells were isolated from draining LNs. LN cells (6×10^6/mL) were cultured in the presence of 50 μg/mL MOG35-55 and 25 ng/mL IL-12 in RPMI 1640 medium containing 2 μM 2-ME, penicillin, streptomycin, and 10% heat-inactivated FBS for 4 d. After harvesting and resuspension in Hank's Balance Saline Solution (HBSS), primed LN cells (1.6×10^7) were transferred (i.p.) into naïve mice to induce experimental autoimmune encephalomyelitis (EAE); LN cells from unrecombined control mice ($S1pr1^{loxP/loxP}$) or conditional mutants for $S1P_1$ in CNS cell lineages ($S1pr1^{loxP/loxP}$; *Nestin-cre*) were transferred into naïve unrecombined control mice ($S1pr1^{loxP/loxP}$). Alternatively, LN cells from unrecombined control mice ($S1pr1^{loxP/loxP}$) were transferred into naïve unrecombined control mice ($S1pr1^{loxP/loxP}$) or conditional mutants ($S1pr1^{loxP/loxP}$; *Nestin-cre*). *Bordetella pertussis* toxin (PTX; 200 ng) was injected into mice on the day of and 2 d after adoptive transfer. Mice were weighed and monitored daily for clinical signs of disease.

Histological Analysis. Cryostat tissue sections (20 μm) were fixed (10 min) in 4% paraformaldehyde (PFA), permeablized in 0.5% Triton X-100, and blocked with 3% BSA. Tissue sections were immunolabeled with anti-CD4 (for CD4-T lymphocytes, 1:200; Serotec) or anti-CD11b (FITC-conjugated primary antibody for microglia or macrophages, 1:200; BD PharMingen) for identifying other cell types in EAE lesion areas. Sections were counterstained with DAPI (5 μg/mL). The images were collected using a fluorescence microscope (Axio Imager D1; Zeiss) equipped with an AxioCam digital camera (Zeiss) and prepared using Adobe Photoshop (version 8.0). For cresyl violet staining, cryostat tissue sections were fixed in 4% PFA and stained with 0.02% cresyl violet (Sigma) in acetate buffer. Sections were dehydrated through a series of increasing ethanol baths, cleared in xylene, and mounted with DPX mountant (Fluka). Images were taken using a bright-field microscope equipped with a 100× oil objective lens and an AxioCam digital camera (Zeiss).

In Situ Hybridization. In situ hybridization was performed to determine presence and localization of $S1P_1$ mRNA in the murine embryonic brain of unrecombined control and CNS $S1P_1$ conditional null mutant ($S1pr1^{loxP/loxP}$; *Nestin-cre*) (2). E13.5 embryos were frozen in Tissue-Tek Optimal Cutting Temperature (OCT) (Ted Pella, Inc., Redding, CA) media, sectioned at 20 mm, fixed with 4% paraformaldehyde, acetylated, and dehydrated through an ethanol series before hybridization with an *S1pr1*-specific, digoxigenin (DIG)-labeled antisense riboprobe generated by run-off transcription. Riboprobes were identified with an alkaline phosphatase-conjugated anti-DIG antibody and visualized by incubating with nitro blue tetrazolium/5-bromo-4-chloro-3-indolyl phosphate (NBT/BCIP) colorimetric substrate. Images were collected using a bright-field microscope equipped with an AxioCam digital camera (Zeiss) and prepared using Adobe Photoshop (version 8.0).

Quantitative Real-Time PCR. Total RNA was isolated from different organ tissues or cultured astrocytes from CNS $S1P_1$ conditional null mutants ($S1pr1^{loxP/loxP}$; *Nestin-cre*) or littermate controls using TRIzol reagent (Invitrogen). Approximately 10 μg of each sample were DNase-treated and primed with oligo(dT) before cDNA synthesis with SuperScript II reverse transcriptase (Invitrogen). Targets including *S1pr1* and cytokines were amplified with iQ sybr green supermix (Bio-Rad) on a Bio-Rad iCycler using gene-specific primer pairs (see *Reverse Transcription Primers*) that flank introns. Gene expression was quantified using the $2^{-\Delta\Delta CT}$ method relative to β-actin.

Isolation of NeuN-Positive Nuclei from Spinal Cord. Whole spinal cords were diced with crossed scalpel blades, incubated in HBSS and 2 mM EGTA on ice for 30 min, then gently triturated, and filtered through a 40-μm filter. Cells were lysed by adding a 1% solution of Nonidet P-40 by drop while gently vortexing. Nuclei were then washed and fixed with 1% paraformaldehyde, blocked with 2.5% BSA/0.1% Triton-X 100, labeled with mouse anti-NeuN antibody (Chemicon) and an anti-mouse–AF488 secondary antibody, and counterlabeled with propidium iodide (10 mg/mL). NeuN-positive nuclei were then isolated with a FACSAria cell sorter and extracted with a genomic DNA extraction kit (Qiagen). PCR was performed as described in Fig. S1*B*.

Semiquantitative RT-PCR. Total RNA was isolated from mouse bone marrow or astrocytes that were isolated from WT mice using TRIzol reagent (Invitrogen). Approximately 10 μg of each sample were used for cDNA synthesis. PCR was used for determining gene expression of sphingosine kinase 1 (Sphk1) and Sphk2 in mouse cortical astrocytes, and cDNA from bone marrow was used as a positive control.

Reverse Transcription Primers. *S1pr1* forward 5′ AGGGAACTTTGCGAGTGAG and reverse 5′ GTTACAGCAAAGCCAGGTCAG; *IL-1β* forward 5' CAACCAACAAGTGATATTCTCCATG and reverse 5′ GATCCACACTCTCCAGCTGCA; *IL-6* forward 5′ GAGGATACCACTCCCAACAGACC and reverse 5′ AAGTGCATCATCGTTGTTCATACA; *IL-17* forward 5′ TCCAGAAGGCCCTCAGACTA and reverse 5′ AGCATCTTCTCGACCCTGAA; *Sphk1* forward 5′ AGTCATGTCCGGTGATGGTC and reverse 5′ CCAGTTGGCCTTGGTAGATG; *Sphk2* forward 5′ ATCTCTGAAGCTGGGCTGTC and reverse 5′ GAAGAAGCGAGCAGTTGAGC; *β-actin* qRT-PCR forward 5′ AGCCTTCCTTCTTGGGTATG and reverse 5′ CTTCTGCATCCTGTCAGCAA; *β-actin* RT-PCR forward 5′ TGGAATCCTGTGGCATCCATGAAAC and reverse 5′ TAAAACGCAGCTCAGTAACAGTCCG.

1. Miller SD, Karpus WJ, Davidson TS (2010) Experimental autoimmune encephalomyelitis in the mouse. *Curr Protoc Immunol*, Chapter 15:15.1.1–15.1.20.

2. Weiner JA, Hecht JH, Chun J (1998) Lysophosphatidic acid receptor gene vzg-1/lpA1/edg-2 is expressed by mature oligodendrocytes during myelination in the postnatal murine brain. *J Comp Neurol* 398:587–598.

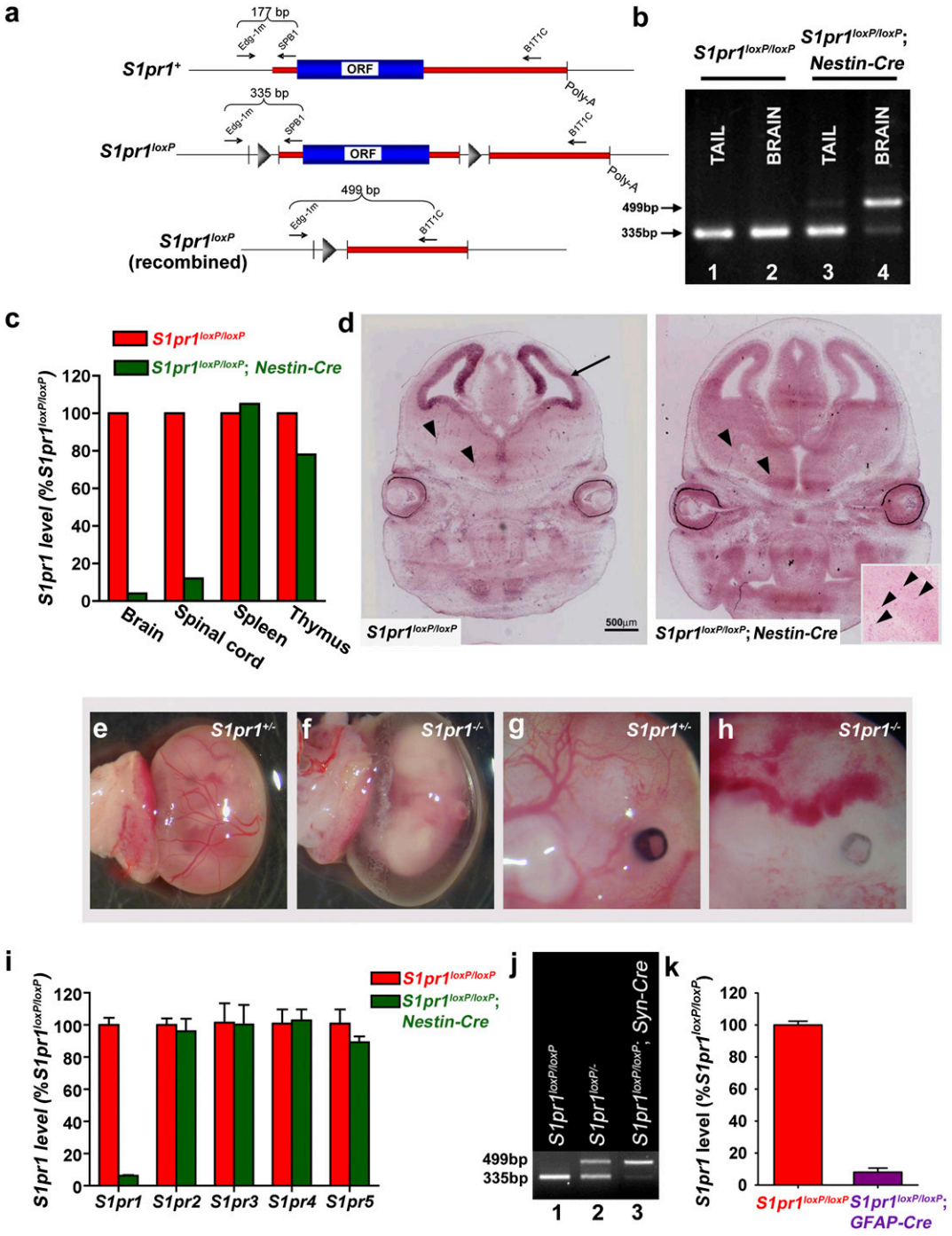

Fig. S1. Tissue-specific deletion of $S1P_1$. (*A*) LoxP sites flanking the ORF of $S1P_1$ were introduced into the genome of ES cells by homologous recombination. Transgenic mice were generated using standard protocols (1). Introduction of Cre recombinase results in the deletion of the entire ORF. (*B*) Gel showing the products of a PCR performed with the three indicated primers (Edg-1m, SPB1, and B1T1C). The 335-bp band shows the presence of the floxed gene, whereas the 499-bp band reveals the recombined KO locus. In the absence of Cre recombinase (lanes 1 and 2), all tissues show only the 335-bp band. When a single copy of Cre driven by the nestin promoter is introduced (lanes 3 and 4), recombination occurs specifically in CNS tissue as shown in the DNA derived from the brain. The faint 499-bp band in lane 3 likely reflects neural cells within the tail preparation, whereas the faint 335-bp band present in the brain in lane 4 is caused by vascular and other non-CNS cell types. (*C*) Loss of CNS $S1P_1$ expression in conditional null mutants (*S1pr1*$^{loxP/loxP}$; *nestin-cre*) with maintained expression in immunological tissues as shown by quantitative real-time PCR. (*D*) In situ hybridization of embryonic brains (E13.5) with an *S1pr1*-specific antisense riboprobe shows abundant expression of *S1pr1* in the proliferative cortical ventricular zone (arrows) that extends into the ganglionic eminence. This expression is completely lost in the KO embryos, which maintain only faint expression throughout the brain in the presumptive vasculature (arrowheads). (*E–H*) To show that the recombined *S1pr1* allele is a true null allele, recombination was performed in germ-line cells. The resulting phenotype confirmed loss of function as reported (2). (*E*) *S1pr1*$^{+/-}$ embryo at day 12.5 after vaginal plug detection (E12.5) showing normal vasculature in the yolk sac. (*F*) *S1pr1*$^{-/-}$ littermate showing absence of blood vessels consistent with the previously reported null allele (2). (*G*) *S1pr1*$^{+/-}$ embryo (E12.5) showing normal vasculature in the head. (*H*) *S1pr1*$^{-/-}$ littermate has extensive intracranial bleeding and embryonic death because of a failure of vascular maturation. (*I*) Quantitative real-time PCR analysis showed that the expression level of all S1P receptors except $S1P_1$ was not statistically different between unrecombined control (n = 3) and conditional null mutants for $S1P_1$ in CNS cell lineages (*S1pr1*$^{loxP/loxP}$; *nestin-cre*; n = 3). (*J*) *S1pr1* is deleted in the majority of *S1pr1*$^{loxP/loxP}$; *Synapsin-cre* neurons. Nuclei from

Legend continued on following page

spinal cord neurons were labeled with an α-NeuN antibody, purified by FACS, and then, analyzed for genomic rearrangement by PCR as described for *B*. *S1pr1*$^{loxP/loxP}$ mice show only the 335-bp floxed allele (lane 1), whereas *S1pr1*$^{loxP/-}$ mice show the predicted roughly equimolar ratio of the 499-bp recombined allele (lane 2). Loss of *S1pr1* is nearly complete in NeuN-positive cells from the spinal cord of *S1pr1*$^{loxP/loxP}$; *Synapsin-cre* mice (lane 3). (*K*) Quantitative real-time PCR analysis showed that $S1P_1$ was conditionally deleted in astrocytes expressing *GFAP-Cre* ($n = 4$) compared with unrecombined controls ($n = 3$). Data in *I* and *J* are expressed as percent of control ± SEM.

1. Contos JJ, Fukushima N, Weiner JA, Kaushal D, Chun J (2000) Requirement for the lpA1 lysophosphatidic acid receptor gene in normal suckling behavior. *Proc Natl Acad Sci USA* 97: 13384–13389.
2. Liu Y, et al. (2000) Edg-1, the G protein-coupled receptor for sphingosine-1-phosphate, is essential for vascular maturation. *J Clin Invest* 106:951–961.

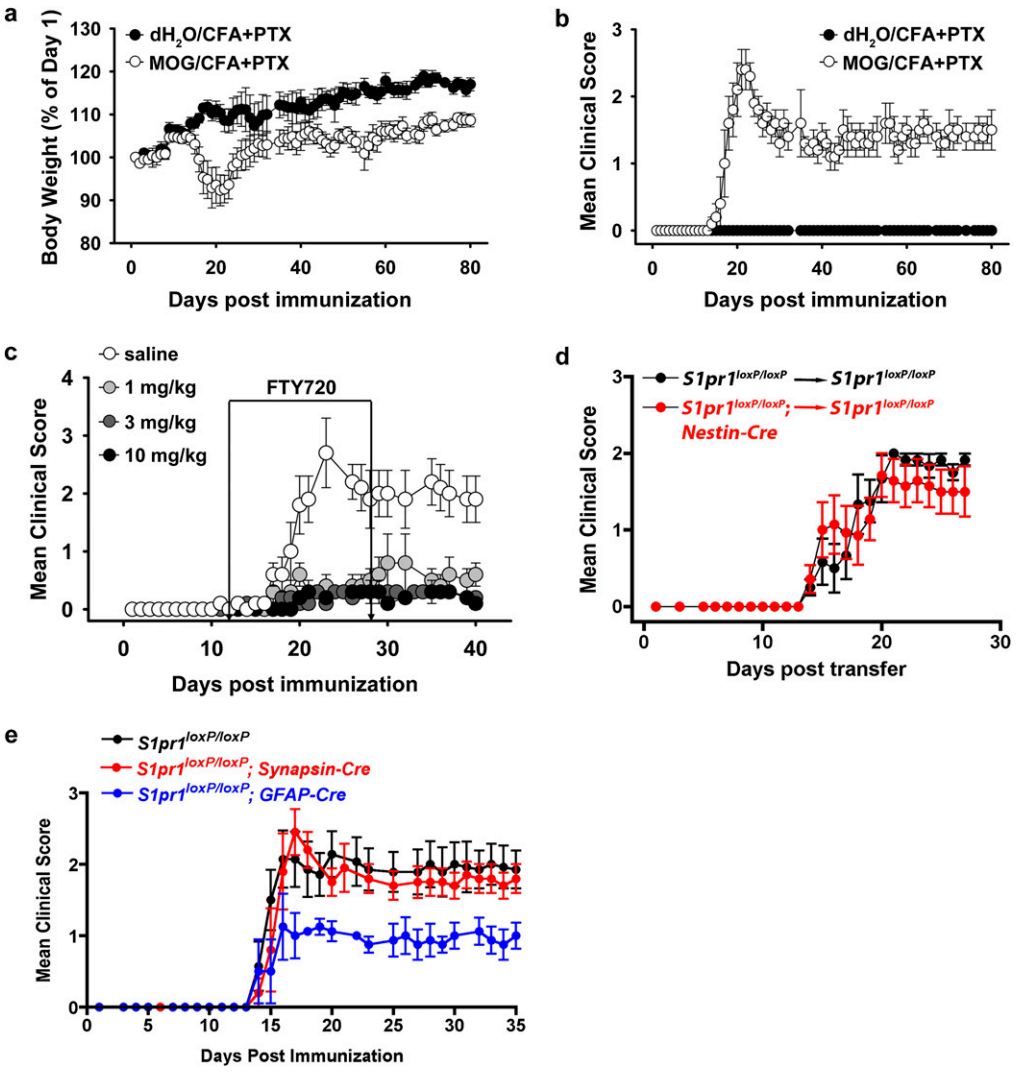

Fig. S2. Monophasic EAE induction. EAE was induced in 7- to 9-wk-old WT mice (C57BL/6J) that were monitored daily. (*A*) Mean body weight. (*B*) Mean clinical score. (*C*) Prevention of EAE was assessed by FTY720 exposure in advance of EAE clinical signs. WT mice challenged with EAE were treated using one-time daily dosing of FTY720 (1 to ∼10 mg/kg, i.p.) starting at day 12 before EAE clinical signs commenced. Controls used saline vehicle solution. Solutions: saline, FTY720 (1 mg/kg), FTY720 (3 mg/kg), and FTY720 (10 mg/kg; $n = 5$ for each group). The box (between days 12 and 28) indicates the period of daily FTY720 administration. (*D*) Normal immunological competence of primed LN cells from both control and conditional nulls for $S1P_1$ in CNS cell lineages during EAE. EAE was induced in 7- to 9-wk-old unrecombined controls (*S1pr1*$^{loxP/loxP}$) or Cre-driven conditional null mutants (*S1pr1*$^{loxP/loxP}$; *nestin-cre*). Primed LN cells from each EAE-induced group were transferred into naïve control mice that were monitored daily. Primed LN cells isolated from both control and conditional null mutant mice induced EAE effectively and similarly [controls into controls ($n = 6$); mutants into controls ($n = 7$)]. Data in all figures are represented as mean ± SEM. (*E*) Response of *S1pr1* conditional nulls to EAE challenge in the absence of FTY720 administration. WT unrecombined mice (*S1pr1*$^{loxP/loxP}$) and mice with neuron-specific deletion of *S1pr1* (*S1pr1*$^{loxP/loxP}$; *Synapsin-Cre*) show similar responses, whereas loss of *S1pr1* from astrocytes (*S1pr1*$^{loxP/loxP}$, *GFAP-Cre*) results in an attenuation of EAE clinical signs. All mice show similar dynamics of disease progression, reaching a plateau by day 20 that is followed by maintenance of a steady disease state.

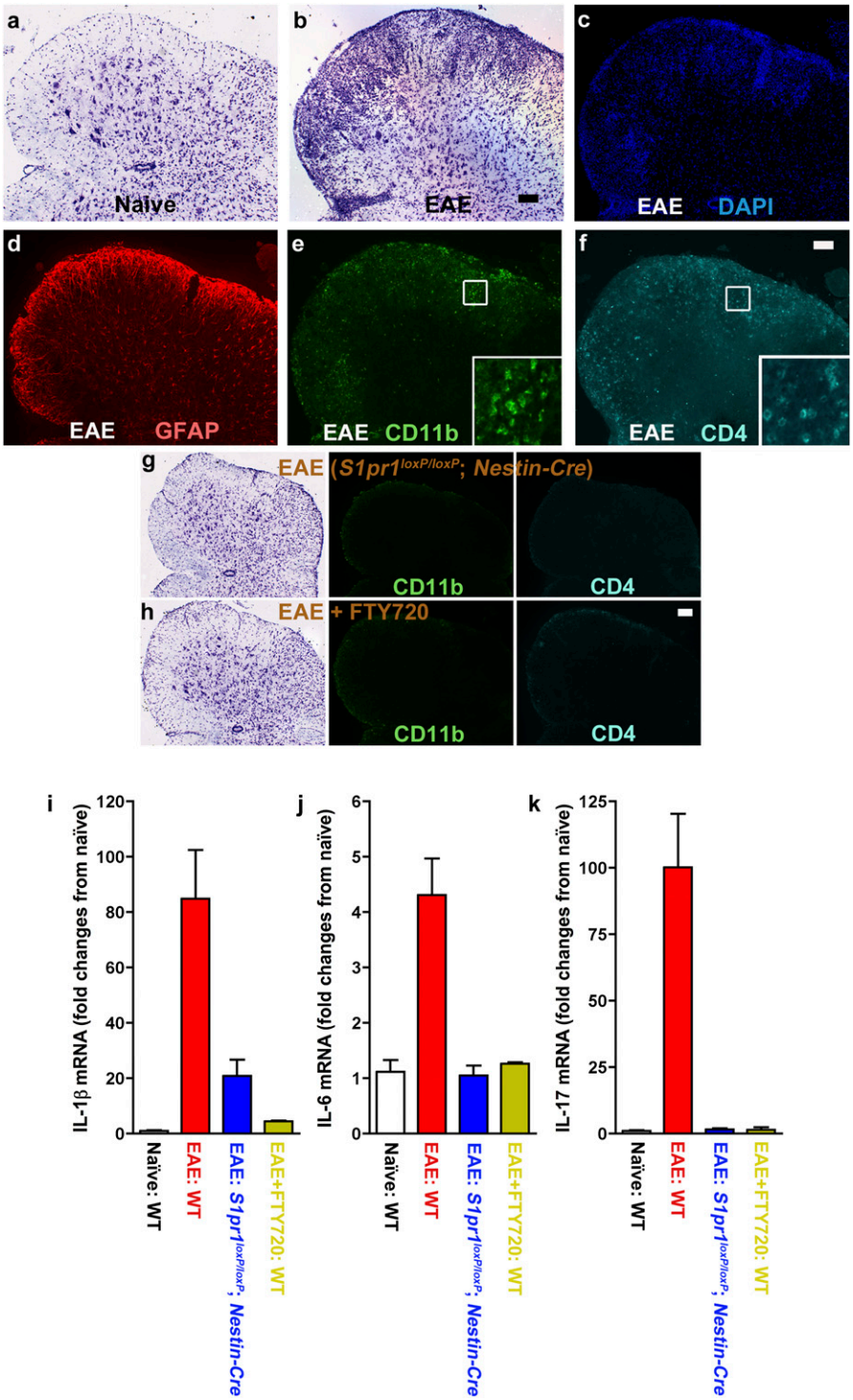

Fig. S3. Cell types in the lumbar spinal cord of EAE lesion areas and immune cell infiltration in EAE-induced conditional null mutants and FTY720-treated mice. (*A* and *B*) Cell population changes in the lumbar spinal cord of naïve (*A*) and EAE (*B*; clinical score at examination = 3) WT mice were determined by cresyl violet staining. Cryostat spinal cord sections (20 μm) of EAE mice were prepared at day 45. (*C*–*F*) Lumbar spinal cords of EAE WT mice (clinical score at examination = 3) were immunolabeled for GFAP (*D*), CD11b (*E*), and CD4 (*F*) cell surface markers corresponding to reactive astrocytes, microglia or macrophages, and lymphocytes, respectively. (*C*) DAPI staining. (*G* and *H*) Cresyl violet staining showed that conditional deletion of $S1P_1$ in CNS cell lineages (*S1pr1*$^{loxP/loxP}$; *Nestin-Cre*; *G*) or FTY720 administration (*H*) markedly prevented or reduced histological sequelae of EAE. Infiltration of CD11b- or CD4-positive immune cells during EAE was reduced by genetic deletion of $S1P_1$ (*G*) and FTY720 administration (*H*). (Scale bar: 100 μm.) (*I*–*K*) Reduction of EAE-induced cytokine levels by genetic $S1P_1$ deletion or FTY720 administration. Cytokine levels (*I*, IL-1β; *J*, IL-6; *K*, IL-17) in the lumbar spinal cord after EAE challenge were reduced in CNS $S1P_1$ conditional null mutants (*S1pr1*$^{loxP/loxP}$; *nestin-cre*) or after FTY720 exposure as measured by quantitative real-time PCR analysis (control gene: β-actin). Data are represented as mean ± SEM.

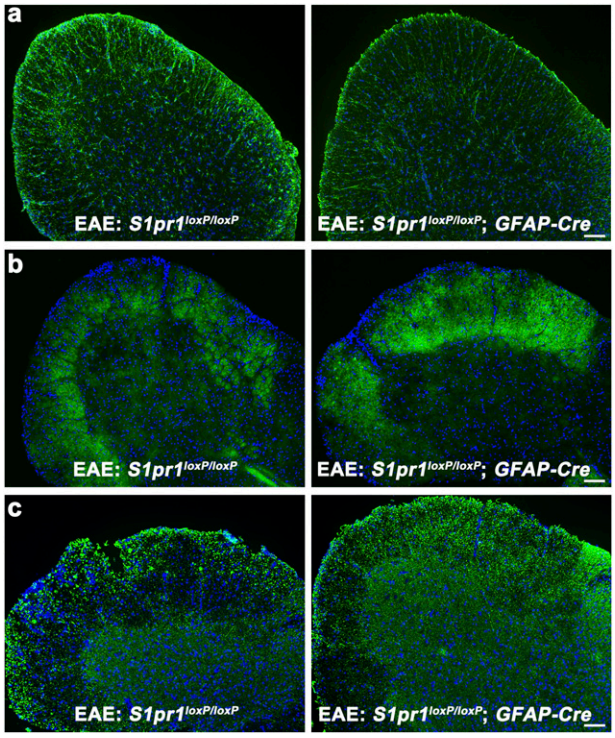

Fig. S4. Reduction of pathological sequelae of EAE by specific $S1P_1$ deletion in GFAP-expressing cells. Astrogliosis (*A*), demyelination (*B*), or axonal damage (*C*) was identified by anti-GFAP immunolabeling, fluoromyelin staining, or antineurofilament immunolabeling in the lumbar spinal cords of EAE-induced controls (*S1pr1*$^{loxP/loxP}$) or GFAP-expressing cell-specific $S1P_1$ conditional null mutants (*S1pr1*$^{loxP/loxP}$; *GFAP-Cre*). (Scale bar: 100 μm.)

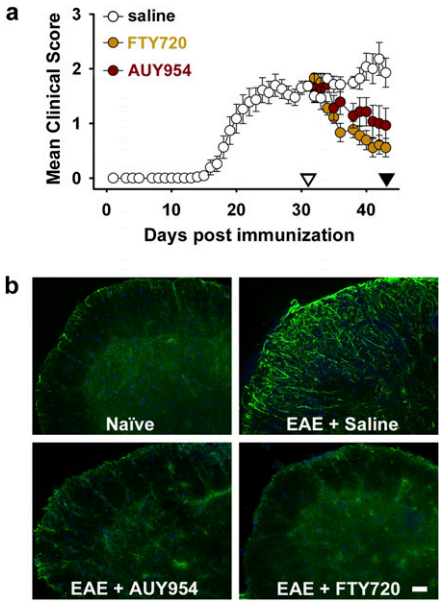

Fig. S5. $S1P_1$ selective agonist, AUY954, reduces astrogliosis and the clinical severity of EAE. (*A*) Mean clinical score of WT EAE challenged with daily treatment of AUY954 (5 mg/kg; $n = 7$) or FTY720 (3 mg/kg; $n = 9$) compared with saline control ($n = 7$). (*B*) Astrogliosis was assessed by anti-GFAP immunolabeling in the lumbar spinal cord. AUY954 reduced astrogliosis to an extent comparable with FTY720 administration. (Scale bar: 50 μm.)

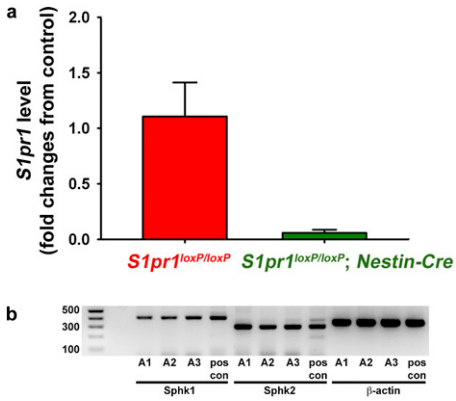

Fig. S6. (*A*) $S1P_1$ is conditionally deleted in astrocytes expressing *Nestin-Cre*. *S1pr1* levels in cortical astrocytes from conditional null mutants (*S1pr1*$^{loxP/loxP}$; *Nestin-Cre*) and littermate unrecombined controls (*S1pr1*$^{loxP/loxP}$) were determined using quantitative real-time PCR. (*B*) Sphk1 and Sphk2 are present in astrocytes. The presence of *Sphk1 and Sphk2* transcripts in cortical astrocytes was determined using semiquantitative RT-PCR. Mouse bone marrow cDNA was used as a positive control. Results shown are from three independent astrocyte cultures (A1, A2, and A3).

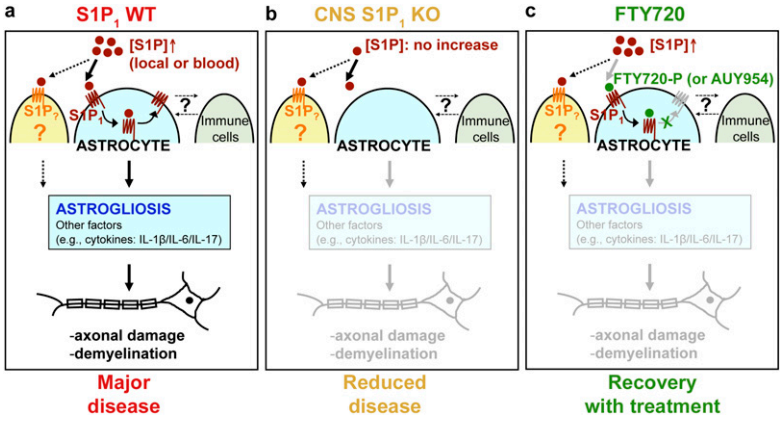

Fig. S7. Schematic diagram summarizing conclusions from this study on the role of CNS $S1P_1$ signaling in the mechanism of action of FTY720. (*A*) The normal progression of EAE, in addition to well-defined immunological components, involves the activation of $S1P_1$ in CNS cell populations, particularly astrocytes, which results in increased $S1P_1$ signaling, including increased levels of S1P itself; this led to astrogliosis that was associated with increases in EAE-relevant cytokine levels, axonal damage, and demyelination. The role of $S1P_1$ signaling in other cell types present in the CNS during EAE as well as signaling mediated by other S1P receptor subtypes in the CNS remains to be determined (signified by a question mark in the orange cell profile). (*B*) Conditional, genetic deletion of $S1P_1$ from CNS cell lineages, particularly astrocytes, reduces disease severity, S1P levels, astrogliosis, and levels of some EAE-relevant cytokines. (*C*) Pharmacological inhibition of $S1P_1$ by functional antagonism (e.g., using FTY720-P or AUY954) also eliminates $S1P_1$ by removal from the cell surface, producing similar effects compared with those in *B*: reductions in astrogliosis, cytokine levels, axonal damage, and demyelination. Immune cells, clearly important for the initiation of EAE, seem to play a lesser role in the mechanism of action for FTY720 using the mouse model compared with CNS $S1P_1$ mechanisms.

Table S1. Lymphocyte levels in blood before and after FTY720 administration

Related figure in manuscript	Group	Lymphocytes (1×10^6 cells/mL) t = 0 h	Lymphocytes (1×10^6 cells/mL) t = 24 h (FTY720)
Fig. 1*B* (normal C57BL/6J)	Naïve	2.57 ± 0.013	0.32 ± 0.026
	EAE	2.98 ± 0.007	0.65 ± 0.076
Fig. 1*D* (Nestin-Cre)	Unrecombined controls–EAE	2.89 ± 0.424	1.052 ± 0.067
	Conditional nulls–EAE	4.99 ± 1.099	1.87 ± 0.467
Fig. 1*F* (Synapsin-Cre)	Unrecombined controls–EAE	2.75 ± 0.396	0.98 ± 0.124
	Conditional nulls–EAE	2.73 ± 0.358	0.99 ± 0.108
Fig. 1*H* (GFAP-Cre)	Unrecombined controls–EAE	2.96 ± 0.470	0.96 ± 0.145
	Conditional nulls–EAE	3.13 ± 0.342	0.74 ± 0.054

Table S2. Statistical analysis (Mann–Whitney's test) for clinical score shown in Fig. 1*A*

	Day	FTY720 (1 mg/kg)	FTY720 (3 mg/kg)	FTY720 (10 mg/kg)	Note
P value of FTY720-administerd group compared with the score when FTY720 administration starts (day 25)	25	0.5368	0.2468	0.5368	FTY720 start
	27	0.4286	0.9307	0.1775	
	28	0.4286	0.9307	0.1775	
	29	0.1255	0.0303	0.0303	
	30	0.0519	0.0303	0.0519	
	31	0.0519	0.0303	0.0173	
	32	0.0303	0.0043	0.0087	
	33	0.1775	0.0173	0.0519	
	35	0.0173	0.0087	0.0043	
	36	0.0173	0.0087	0.0043	
	37	0.0173	0.0087	0.0043	
	38	0.0173	0.0087	0.0043	
	39	0.0173	0.0087	0.0043	
	40	0.0087	0.0043	0.0043	
	41	0.0303	0.0087	0.0043	
	42	0.0087	0.0043	0.0043	
	43	0.0303	0.0087	0.0043	FTY720 stop

Table S3. Statistical analysis (Mann–Whitney's test) for clinical score shown in Fig. 1*C*

	Day	Mutant	Control	Mutant	Note
P value of KO compared with control	16	0.8478			
	17	0.9537			
	20	0.019			
	21	0.0242			
	22	0.0257			
	23	0.0218			
	24	0.0416			
	26	0.0456			
	27	0.0416			
	28	0.0155			
	29	0.0074			
	31	0.0213			
P value of FTY720-administered group compared with the score when FTY720 administration starts (day 34)	34				FTY720 start
	35		0.9551	0.8633	
	36		0.7789	0.7304	
	37		0.7789	0.3401	
	38		0.0401	0.8633	
	41		0.0012	0.4363	
	42		0.0093	0.8633	
	44		0.0006	0.7304	
	45		0.0012	0.7304	
	48		0.0003	0.8633	
	50		0.0003	0.2581	
	51		0.0003	0.6048	
	53		0.0003	0.8633	
	54		0.0003	0.9314	FTY720 stop

Table S4. Statistical analysis (Mann–Whitney's test) for clinical score shown in Fig. 1*E*

	Day	Mutant	Control	Mutant	Note
P value of KO compared with control	16	0.266			
	17	0.2088			
	18	0.5166			
	20	0.4317			
	21	0.3106			
	23	0.8218			
	25	1			
	27	0.6009			
	28	0.9701			
P value of FTY720-administered group compared with	29				FTY720 start
the score when FTY720 administration starts (day 29)	30		0.9015	0.6616	
	31		0.535	0.2901	
	32		0.1649	0.036	
	33		0.053	0.0267	
	34		0.007	0.0054	
	35		0.007	0.0022	
	36		0.0041	0.0019	
	37		0.0111	0.0016	
	39		0.0023	0.0012	
	41		0.0023	0.0012	
	41		0.007	0.0005	
	42		0.0041	0.0004	
	43		0.0041	0.0004	FTY720 stop

Table S5. Statistical analysis (Mann–Whitney's test) for clinical score shown in Fig. 1*G*

	Day	KO	Control	KO	Note
P value of KO compared with control	13	0.3436			
	14	0.3186			
	15	0.4349			
	16	0.6145			
	17	0.343			
	18	0.3577			
	19	0.1472			
	20	0.085			
	21	0.0748			
	22	0.0314			
	23	0.0705			
	24	0.0447			
	25	0.0142			
	26	0.0016			
	27	0.0033			
	28	0.0012			
	29	0.0009			
P value of FTY720-administered group compared with	30				FTY720 start
the score when FTY720 administration starts (day 30)	31		0.0664	0.8846	
	32		0.0019	0.6221	
	33		0.0002	0.9076	
	34		<0.0001	0.9075	
	35		<0.0001	1	
	36		<0.0001	1	
	37		<0.0001	0.8618	
	38		<0.0001	0.9076	
	39		<0.0001	1	
	40		<0.0001	0.9076	
	41		<0.0001	0.9078	
	42		<0.0001	0.9076	
	43		<0.0001	0.9076	
	44		<0.0001	1	FTY720 stop